Eur Biophys J (2004) 33: 360–369
DOI 10.1007/s00249-003-0367-y

ARTICLE

Jae Boum Youm · Yung E. Earm · Won-Kyung Ho

Modulation of HERG channel inactivation by external cations

Received: 8 August 2003 / Revised: 30 September 2003 / Accepted: 30 September 2003 / Published online: 29 October 2003

Abstract We investigated the effect of external cations on the permeability characteristics and gating kinetics of the human *ether-à-go-go*-related gene (HERG) current using the whole-cell patch-clamp technique. Inward HERG currents were recorded on hyperpolarization in 140 mM external Cs^+ and Rb^+, as well as K^+. The permeability ratios of Rb^+ and Cs^+ relative to K^+ were 1.25 and 0.56, respectively. Biphasic outward currents were recorded on depolarization in 140 mM Cs^+ and in Rb^+ with much smaller amplitude. The voltage dependence of inactivation was affected by external cations, such that the half-inactivation voltage shifted from -69.4 ± 3.7 mV in K^+ to -30.7 ± 1.6 mV in Cs^+ and to -35.8 ± 1.9 mV in Rb^+ ($n = 5$). The time constants of inactivation were also changed significantly by external cations; τ of inactivation at $+40$ mV was 16.4 ± 2.2 ms in 140 mM K^+, 181 ± 20.3 ms in Cs^+, and 94.1 ± 7.6 ms in Rb^+ ($n = 5$). Voltage dependence of activation was not altered significantly. The inhibition of the rapid inactivation mechanism by large cations may suggest that the "foot-in-the-door" model of gating is involved in HERG channel inactivation.

Keywords Caesium · Cation permeability · Human *ether-à-go-go*-related gene · Inactivation · Rubidium

Y. E. Earm · W.-K. Ho (✉)
Department of Physiology and Biophysics,
Seoul National University College of Medicine,
28 Yonkeun-Dong,
Chongno-Ku,
110-799 Seoul, Korea
E-mail: wonkyung@snu.ac.kr
Tel.: +82-2-7408227
Fax: +82-2-7639667

J. B. Youm
Department of Physiology,
Cheju National University College of Medicine,
1 Ara 1-Dong,
690-756 Jeju, Korea

Introduction

The human *ether-à-go-go*-related gene (HERG) is known to encode a K^+ channel that has electrophysiological properties similar to those of the rapidly activating delayed rectifier K^+ current (I_{Kr}), which has been described in rabbit, guinea pig, and human heart (Escande et al. 1987; Ho et al. 1996; Sanguinetti and Jurkiewicz 1990; Sanguinetti et al. 1995; Shibasaki 1987; Trudeau et al. 1995). Genetic defects in the HERG gene are associated with congenital and acquired long QT syndrome (Curran et al. 1995), a disease characterized by an unusually slow repolarization of the cardiac action potential and an increased risk of life-threatening cardiac arrhythmias.

A hallmark of HERG channels that distinguishes them from other voltage-gated potassium channels such as the *Drosophila* and mammalian voltage-gated potassium channels (K_v) and the *ether-à-go-go* gene (*eag*) family of potassium channels is a strong inward rectification. As a result, K^+ conductance is small during the plateau phase of the cardiac action potential, but it increases during phase III repolarization. This behaviour is remarkable considering that the HERG protein has a high degree of homology to outwardly rectifying members of the *eag* family (Schönherr and Heinemann 1996).

The mechanism of inward rectification has been investigated in other studies (Smith et al. 1996; Spector et al. 1996). Unlike typical inward rectifier K^+ channels where rectification is caused by voltage-dependent blocking by intracellular Mg^{2+} and polyamines, HERG channels show rectification by a very rapid inactivation ($\tau < 20$ ms) that develops at far more negative potentials ($V_{1/2} = -85$ mV) (Schönherr and Heinemann 1996; Smith et al. 1996; Spector et al. 1996; Zou et al. 1998). Mutagenesis studies have identified that HERG mutation in the pore-loop and in the N-terminal half of the S6 domain can disrupt the fast inactivation process (Fan et al. 1999; Hoshi et al. 1991; Schönherr and Heinemann 1996; Smith et al. 1996; Zou et al. 1998). These are

equivalent to the positions that are important for *Shaker*'s C-type inactivation. Cysteine accessibility experiments with *Shaker* channels suggest that conformational rearrangements in the outer mouth of the pore mediate C-type inactivation (Liu et al. 1996; Yellen 1998). In contrast, N-type inactivation is derived from the occlusion of the inner vestibule by the cytoplasmic NH_2-terminal "ball" (Hoshi et al. 1990; Zagotta et al. 1990). Despite the similarity in structural elements involved in the C-type inactivation between HERG and *Shaker*, the inactivation of HERG is much faster than *Shaker*'s C-type inactivation (Fan et al. 1999).

Slowing of inactivation by raising the concentration of external K^+ or TEA^+ has been considered a characteristic feature of C-type inactivation in the *Shaker* K^+ current (Choi et al. 1991; Hoshi et al. 1990, 1991; Lopez-Barneo et al. 1993). The effect of K^+ was shown to be mimicked by Rb^+, but with much less potency by the less permeant ions Na^+, Cs^+, and NH_4^+ (Lopez-Barneo et al. 1993; Swenson and Armstrong 1981). The "foot-in-the-door" model of gating has been used to explain these results; according to this model, the permeant cation interacts with amino acids in the ion-conducting pore, physically preventing the closing of the outer mouth of the channel protein (Baukrowitz and Yellen 1996; Ruben and Thompson 1984; Swenson and Armstrong 1981). The slowing of inactivation by increasing $[K^+]_o$ and $[TEA^+]_o$ were also observed in HERG K^+ currents (Smith et al. 1996; Wang et al. 1996, 1997), but it is not yet clear whether the modulation of HERG inactivation by external cations shares the same mechanism with the *Shaker* K^+ channel. To further understand these processes, it is necessary to investigate the permeability characteristics of other monovalent cations such as Cs^+ and Rb^+ and their effects on the inactivation mechanism.

In the present study, we investigated the permeability characteristics and gating kinetics of the HERG current in various ionic conditions. The permeability ratios of Rb^+ and Cs^+ relative to K^+ were 1.25 and 0.56, respectively. The inactivation was significantly slowed by Cs^+ and, with less potency, by Rb^+. The voltage dependence of steady-state inactivation was also shifted significantly by Rb^+ and Cs^+ without significant changes in the voltage dependence of activation.

Portions of this work were previously published in abstract form (Youm et al. 1999).

Materials and methods

Expression of HERG in CHO cells

Chinese hamster ovary (CHO) cells were seeded at low density (25,000 cells/35-mm dish) for 2 days prior to transfection. CHO cells were maintained in MEM media supplemented with 10% foetal calf serum and penicillin/streptomycin at 37 °C under 5% CO_2. CHO cells were cotransfected with HERG and green fluorescent protein (GFP) (Clontech) in pcDNA3.1 using Lipofectamine Plus (Life Technologies) transfection reagent (Marshall et al. 1995). Green fluorescence from the GFP-expressing cells was identified using a Nikon microscope equipped with excitation and barrier filters and a mercury lamp light source. Cells were used 2 days after transfection.

Electrophysiological recordings and data analysis

The standard whole-cell voltage-clamp method (Hamill et al. 1981) was performed using an Axopatch-1C amplifier (Axon Instruments, Calif., USA). Recording pipettes were fabricated and fire polished from 1.5 mm o.d. glass (Clark Electromedical, UK) to produce microelectrodes with resistances of 2–4 MΩ when filled with K^+-rich recording solution. A giga seal was made by applying negative pressure at approximately −20 cm H_2O, and seal resistance was usually above 2 GΩ. The current signals were filtered via a 1–10 kHz, 4-pole Bessel-type low-pass filter and digitized using Digidata 1200 (Axon Instruments) for subsequent analysis (pCLAMP software 6.0.1, Axon Instruments). In most experiments, the temperature was set at room temperature (~20–24 °C). All averaged and normalized data are presented as mean ± SEM. Significant differences were detected using Student's unpaired *t*-test ($P < 0.05$). The reversal potentials were determined in each cell as the zero current intercept of the polynomial fit (4-order) to the current–voltage relationship.

Solutions

Normal Tyrode solution contained (in mM) 143 NaCl, 5.4 KCl, 0.5 $MgCl_2$, 1.8 $CaCl_2$, 5.5 glucose, and 5 HEPES. Isotonic K^+ solutions contained 140 KCl, 2 $MgCl_2$ (to eliminate surface charge effects), 10 HEPES, and 5.5 glucose (pH adjusted to 7.4). Isotonic Cs^+ or Rb^+ bath solutions were made by substituting K^+ with the same concentration of Cs^+ or Rb^+. Recording pipettes contained 140 KCl (depending on experiments) with 5 EGTA, 10 HEPES, 5 MgATP, 2.5 diTris-phosphocreatine, and 2.5 disodium phosphocreatine (pH 7.2). CsOH was purchased from Aldrich (USA) and all other chemicals were from Sigma.

Results

Permeability characteristics of the HERG channel expressed in CHO cells

CHO cells expressing HERG were tested to compare the effects of 140 mM K_o^+, Cs_o^+, and Rb_o^+ on the gating and permeability characteristics of the HERG channel. As shown in Fig. 1A, step hyperpolarizing pulses were applied between −100 and −10 mV in 10 mV increments for 3.2 s from a holding potential of +30 mV. Under all ionic conditions, hyperpolarization induced a current that showed a typical time course and inward rectification that are known to be characteristic of HERG (Smith et al. 1996; Spector et al. 1996), indicating that Cs^+ and Rb^+ as well as K^+ can permeate through HERG channels. When the peak amplitudes of the current measured at −80 mV in Cs_o^+ and Rb_o^+ were normalized to that in K_o^+, they were 0.66 ± 0.10 ($n = 7$) and 1.19 ± 0.08 ($n = 6$), respectively. On return to the holding potential of +30 mV, the current response in Cs_o^+ was distinct from that of others. In 140 mM K_o^+ (Fig. 1A, upper panel) or Rb_o^+ (Fig. 1A, middle panel), time-dependent outward tail currents were hardly observed, which is due to the rapid inactivation, a

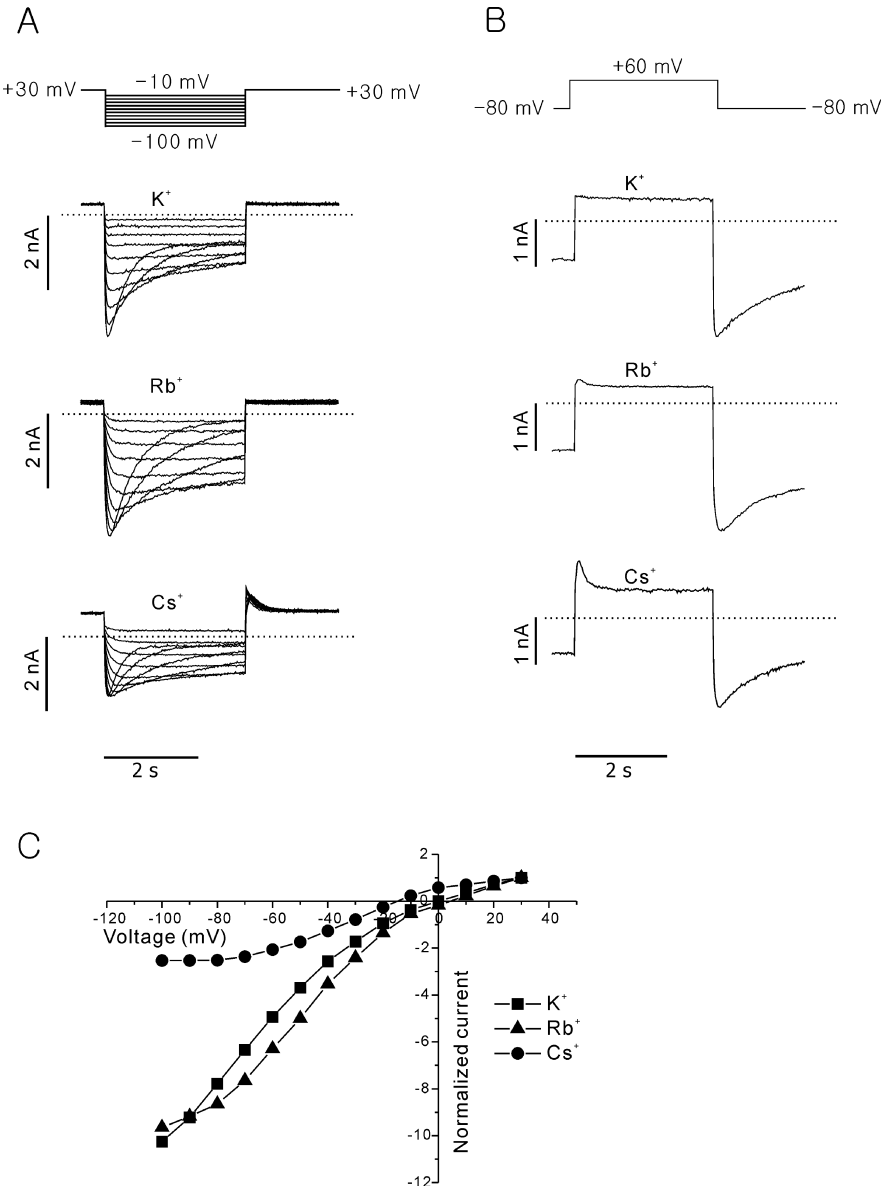

Fig. 1A–C HERG currents recorded in various ionic conditions. Bath solutions contained 140 mM K^+ (*upper panel*), Rb^+ (*middle panel*), and Cs^+ (*lower panel*). $[K^+]_i = 140$ mM. **A** Superimposed current traces evoked by step hyperpolarization between −100 and −10 mV in 10 mV increments for 3.2 s from a holding potential of +30 mV. **B** Membrane currents were evoked by a 3.2 s depolarizing pulse to +60 mV from a holding potential of −80 mV. **C** Current–voltage (*I–V*) relationships for the normalized amplitude of peak current at step hyperpolarization. Peak current amplitude was normalized to the amplitude at +30 mV. Actual current amplitude at +30 mV was measured as 286 pA for K^+, 310 pA for Rb^+, and 631 pA for Cs^+

well-known characteristic of HERG. In 140 mM Cs^+_o, however, a significant amount of outward K^+ currents was observed on return to the holding potential (Fig. 1A, lower panel). When the depolarization potential was increased to +60 mV, small but distinct time-dependent outward currents were observed in Rb^+_o as well as in Cs^+_o (Fig. 1B, middle and lower panels). In K^+_o, however, a time-dependent component of outward currents was still not observed (Fig. 1B, upper panel).

Peak current–voltage relationships were obtained by measuring the peak current amplitude at step hyperpolarization. The amplitude was normalized to the value at +30 mV and plotted as a function of the voltage at step hyperpolarization (Fig. 1C). The result shows that HERG currents in Cs^+_o have less inward rectification than those in Rb^+_o or K^+_o. From the reversal potentials, the permeability ratios of Rb^+ and Cs^+ relative to K^+ (P_{Rb}/P_K, P_{Cs}/P_K) were calculated according to the Goldman–Hodgkin–Katz voltage equation. The reversal potentials were $+5.7 \pm 1.1$ mV for Rb^+_o ($n = 4$) and -15 ± 1.6 mV for Cs^+_o ($n = 4$), and calculated values for P_{Rb}/P_K and P_{Cs}/P_K were 1.25 and 0.56, respectively (Hille 1992).

Voltage dependence of activation and inactivation in the HERG channel

Considering that the inward rectification of HERG currents is caused by rapid inactivation kinetics (Smith et al. 1996; Spector et al. 1996), the above results suggest that the inactivation mechanism is affected by the external cation species. To determine the effect of external cation species on the inactivation mechanism, steady-state inactivation curves were obtained in various ionic conditions using a three-step voltage-clamp

protocol (Fig. 2A) (Sanchez-Chapula and Sanguinetti 2000). From a holding potential of 0 mV, a 3 s depolarizing prepulse to +60 mV was applied, followed by step hyperpolarization between −120 and +30 mV in 10 mV increments, and then a final pulse to +30 mV. The peak outward tail current was estimated by extrapolating the current trace back to beginning of the third pulse and by fitting the time course with a single exponential function. The amplitude of the peak current was then normalized to the value of maximum amplitude and plotted as a function of the voltage at step hyperpolarization. Data were fitted to the Boltzmann equation to obtain the half-inactivation voltage ($V_{1/2}$) and the slope factor (k). The value of $V_{1/2}$ in K_o^+, Rb_o^+, and Cs_o^+ was -69.4 ± 3.7, -35.8 ± 1.9, and -30.7 ± 1.6 mV ($n=5$), respectively. The slope factor was also affected by external cation species; the slope factor was 28.8 ± 3.3, 22.2 ± 2.1, and 18.8 ± 1.6 mV for K_o^+, Rb_o^+, and Cs_o^+, respectively (Fig. 2C).

The voltage dependence of current activation was assessed using standard tail current analysis (Fig. 3A). Currents were elicited using 5 s test pulses between −70 and +70 mV in 10 mV increments, every 60 s from a holding potential of −90 mV. Tail currents were recorded on return to the holding potential of −90 mV, where the inactivation recovers quickly and then the deactivation follows slowly. They were fitted with a two-exponential function and the current amplitudes were extrapolated back to the beginning of the repolarizing pulse. Their amplitudes were normalized to the value of maximum amplitude among them. Normalized current amplitudes were then plotted as a function of test pulse potential, and the data were fitted with the Boltzmann equation. As shown in Fig. 3B, there was no significant difference among the half activation voltages ($V_{1/2}$) in 140 mM K_o^+ ($V_{1/2}=-18.9 \pm 4.1$ mV, $n=5$), Rb_o^+ ($V_{1/2}=-17.7 \pm 2.9$ mV, $n=3$), or Cs_o^+ ($V_{1/2}=-15.9 \pm 2.7$ mV, $n=5$).

Activation and inactivation time constants in the HERG channel

We also assessed the effect of external cation species on the rate of inactivation. Because inactivation was slower than activation in Cs_o^+ solution, the rate of inactivation could be directly measured from the current traces elicited by depolarizing voltage step pulses between +10

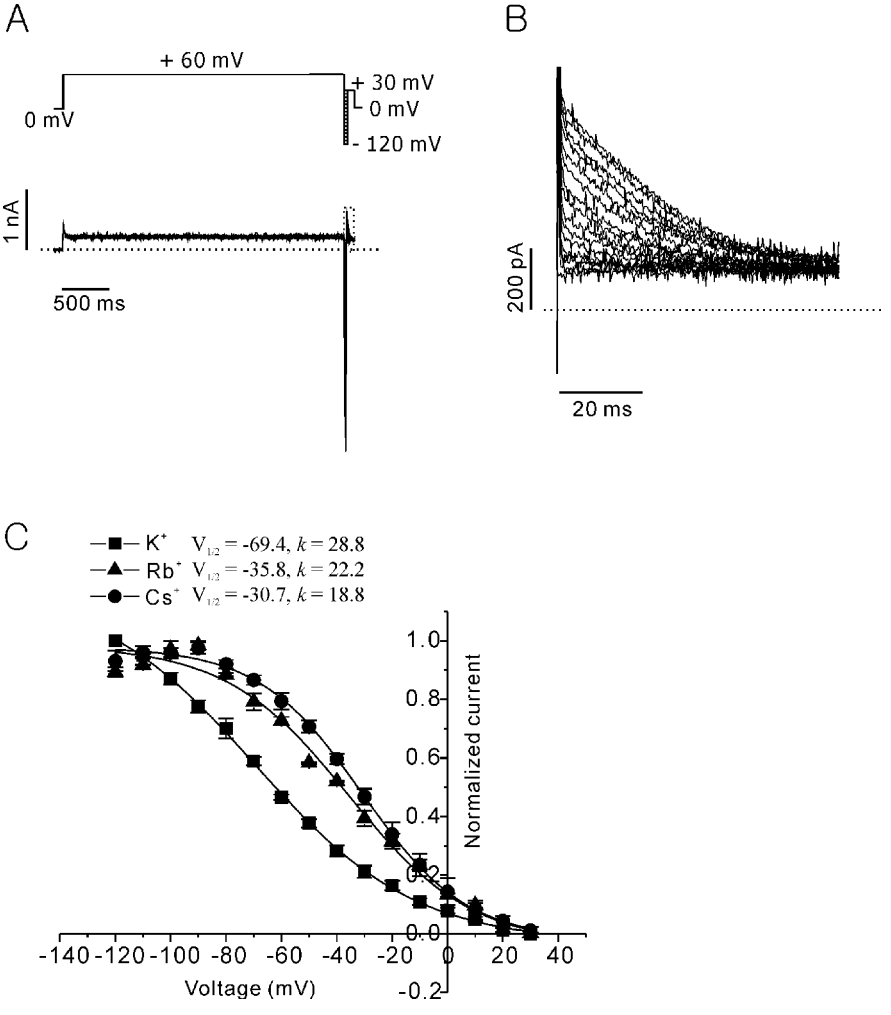

Fig. 2A–C Effects of external cations on the voltage dependence of steady-state inactivation. Bath solutions contained 140 mM K^+ (*filled squares*), Rb^+ (*filled triangles*), or Cs^+ (*filled circles*). $[K^+]_i = 140$ mM. **A** A three-step voltage-clamp protocol and the membrane currents for 140 mM $[K^+]_o$ are shown: first step to +60 mV for 3 s; second step of hyperpolarizing test pulses between −120 and +30 mV in 10 mV increments for 20 ms; third step to +30 mV for 100 ms. Holding potential = 0 mV. **B** Expanded view of currents outlined by dotted box in **A**. **C** Voltage dependence of HERG inactivation. The differences between amplitudes of peak and steady-state tail current were normalized to their maximum value, and then were plotted against the test potentials. Data were well-fitted by a Boltzmann equation ($I/I_{max} = 1/(1+\exp\{(V_{1/2}-V_m)/k\})$. The *symbols with error bars* represent mean ± SEM; data were obtained from five cells

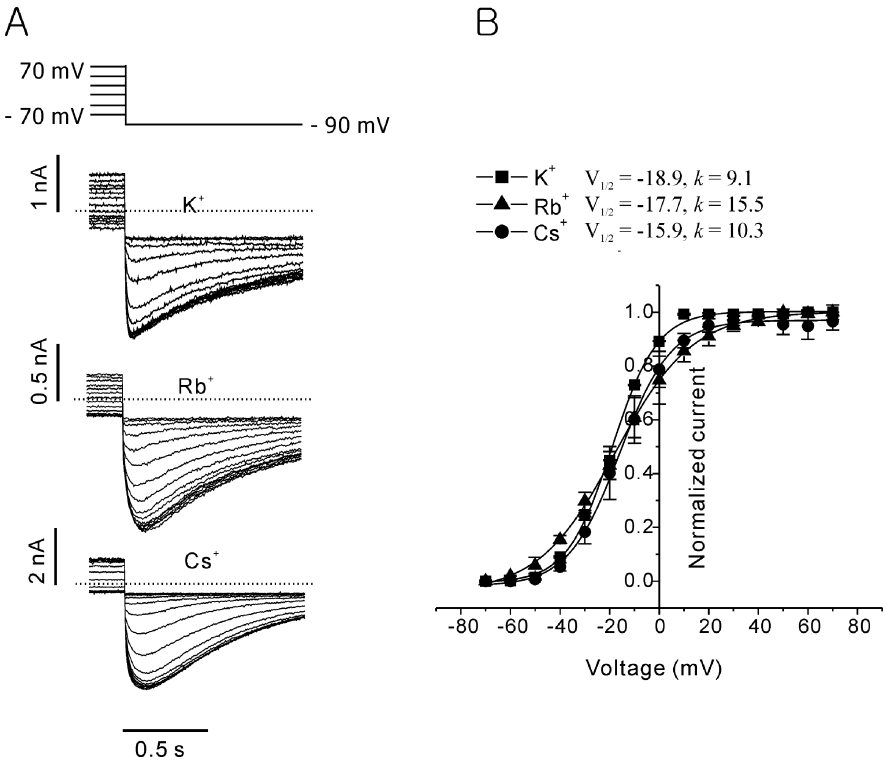

Fig. 3A, B Effects of external cations on the voltage dependence of steady-state activation. Bath solution contains 140 mM K^+ (*filled squares*), Rb^+ (*filled triangles*), or Cs^+ (*filled circles*). $[K^+]_i$ is 140 mM. **A** Currents were evoked by 5 s step pulses between −70 and +70 mV in 10 mV increments and returned to a holding potential of −90 mV. **B** Voltage dependence of HERG channel activation. The differences between amplitudes of peak and steady-state tail current were normalized to their maximum value, and then were plotted against the test potentials ($n = 3$–5)

and +60 mV from a holding potential of −80 mV (Fig. 4A, left panel). Rates of both activation and inactivation appeared to become faster with larger depolarization. Biphasic current traces were fitted to a multiplication of two monoexponential functions, and time constants for both inactivation and activation were obtained. In K_o^+ or Rb_o^+ solution, we used the three-step voltage-clamp protocol (Fig. 4A, middle and right panels) (Sanchez-Chapula and Sanguinetti 2000) to resolve the fast rate of inactivation at depolarizing membrane potentials. An initial 3 s pulse to +60 mV was applied from a holding potential of −80 mV. A second pulse of −130 mV was applied (20 ms for K_o^+, 80 ms for Rb_o^+) to allow sufficient time for channels to recover from inactivation without significant deactivation. Then, step depolarizations ranging between +10 and +60 mV in 10 mV increments were applied to obtain the time constant of inactivation at each step pulse potential. The current during the final step depolarization was fitted by a single exponential function to determine the rate of fast inactivation. Cs_o^+ and Rb_o^+ slowed the rate of inactivation significantly, and the effect of Cs_o^+ was stronger than that of Rb_o^+ (Fig. 4B).

The rates of recovery from inactivation and deactivation in Cs_o^+, Rb_o^+, and K_o^+ were assessed by step hyperpolarization from a holding potential of +30 mV (see Fig. 1A). The resulting current traces showed a rapid development of inward current due to recovery from inactivation (Fig. 5A, left panel), followed by a much slower decay due to deactivation (Fig. 5B, left panel). Each trace was fitted with a multiplication of two monoexponential functions. Rates of recovery from the inactivation and deactivation were then plotted as a function of membrane potential in Fig. 5 (A, right panel shows recovery from inactivation; B, right panel shows deactivation). The rate of recovery from inactivation was significantly slower in Rb_o^+ ($P < 0.01$) and Cs_o^+ ($P < 0.01$) than in K_o^+. The rate of deactivation in Cs^+ was faster than that in K^+ or Rb^+. For example, τ at −80 mV increased from 976.2 ± 80.5 ms in Cs_o^+ to 1644.6 ± 250.9 ms in K_o^+ ($n = 5$, $P < 0.01$) and to 1746.7 ± 148.2 ms in Rb_o^+ ($n = 5$, $P < 0.01$).

Discussion

One of the major findings in the present study is that external cation species modulate the kinetics of the HERG current by affecting the inactivation mechanism. It is generally accepted that HERG is activated by depolarization, while at the same time it is even more rapidly inactivated (Smith et al. 1996; Spector et al. 1996). Therefore, HERG in an isotonic K^+ solution was well recognized as inward currents by hyperpolarizing voltage steps, whereas outward currents by depolarizing voltage steps were negligible (Fig. 1A, upper panel). In isotonic Rb^+ or Cs^+ solutions, however, time-dependent currents developed both in outward and inward directions (Fig. 1B). The time course of outward Cs^+ currents (Fig. 4A, left panel) clearly demonstrates that inactivation at a depolarized potential is significantly slower than activation. A plausible interpretation of the result is that Rb_o^+ and Cs_o^+ revealed the time-dependent component of outward currents more clearly by slowing

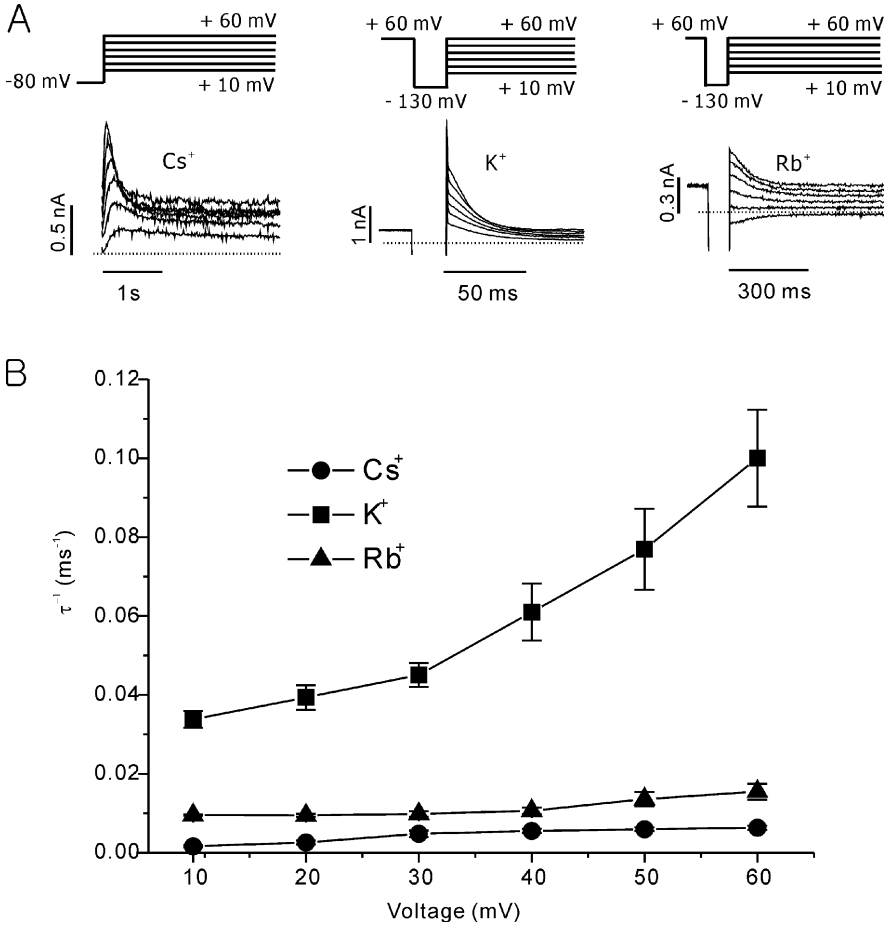

Fig. 4A, B Effects of external cations on the kinetics of inactivation. **A** Current traces showing the kinetics of inactivation. For Cs_o^+, time constants of inactivation were assessed by applying test pulses between +10 and +60 mV in 10 mV increments from a holding potential of –80 mV (*left panel*). Resulting currents had a rapid rising phase (activation) followed by a much slower decay phase (inactivation), and were fitted with a two-exponential function. For K_o^+ and Rb_o^+, a three-step voltage-clamp protocol was used to resolve the fast rate of inactivation at depolarizing membrane potentials (*middle and right panels*). An initial 3 s pulse to +60 mV was applied from a holding potential of –80 mV. A second pulse of –130 mV was applied (20 ms for K_o^+, 80 ms for Rb_o^+). Then, step depolarizations ranging between +10 and +60 mV in 10 mV increments were applied to find the time constant of inactivation. **B** The voltage dependence of inactivation rate (reciprocals of inactivation time constants) in bath solutions containing 140 mM Cs_o^+ (*filled circles*), $K^+{}_o$ (*filled squares*), or $Rb^+{}_o$ (*filled triangles*) ($n = 3$–5)

inactivation. The TEA_o^+ also interferes with inactivation of HERG channels, resulting in biphasic outward currents with similar kinetics to those observed in Cs_o^+ (Smith et al. 1996). Considerable slowing of inactivation by TEA_o^+ or K_o^+ was also found in *Shaker* B channels (Choi et al. 1991). It has been proposed that the rate of C-type inactivation is controlled by the dwell time of the last ion at one of the K^+ binding sites (Baukrowitz and Yellen 1996). From the studies of the chimeric K^+ channel (Kv2.1/1.3), a model was proposed whereby C-type inactivation involves a constriction at the selectivity filter, which cannot proceed when the selectivity filter is occupied by K^+ (Kiss and Korn 1999). This model implies that permeant cations bind to a selectivity filter in the HERG channel, which is very flexible, and that the off-rate of permeant cations determines the rate of inactivation. Interestingly, the potency of this effect on the inactivation mechanism was $Cs^+ > Rb^+ > K^+$, a sequence corresponding to the size of ions. This result may imply that the physically larger Cs^+ could prevent constriction more effectively than smaller K^+ and Rb^+. One report supporting this idea, which used experiments on human channel hKv1.5, suggested that ions with a larger crystal radius impede inactivation when they are permeating the channel (Fedida et al. 1999).

Recently, the effects of Cs_o^+ and K_o^+ on inactivation of HERG channels were also described by Zhang et al. (2003). They found that replacement of 5 mM K_o^+ by 135 mM Cs_o^+ increased both inactivation and recovery time constants and shifted the midpoint of the steady-state inactivation curve by 25 mV in the depolarized direction without affecting activation. In our study, replacement of 140 mM K_o^+ by 140 mM Cs_o^+ also increased inactivation time constants and shifted the midpoint of the steady-state inactivation curve by 39 mV. The difference in the degree of shift is believed to come from the different concentrations of K_o^+ used in the two experiments. As for activation, the voltage depen-

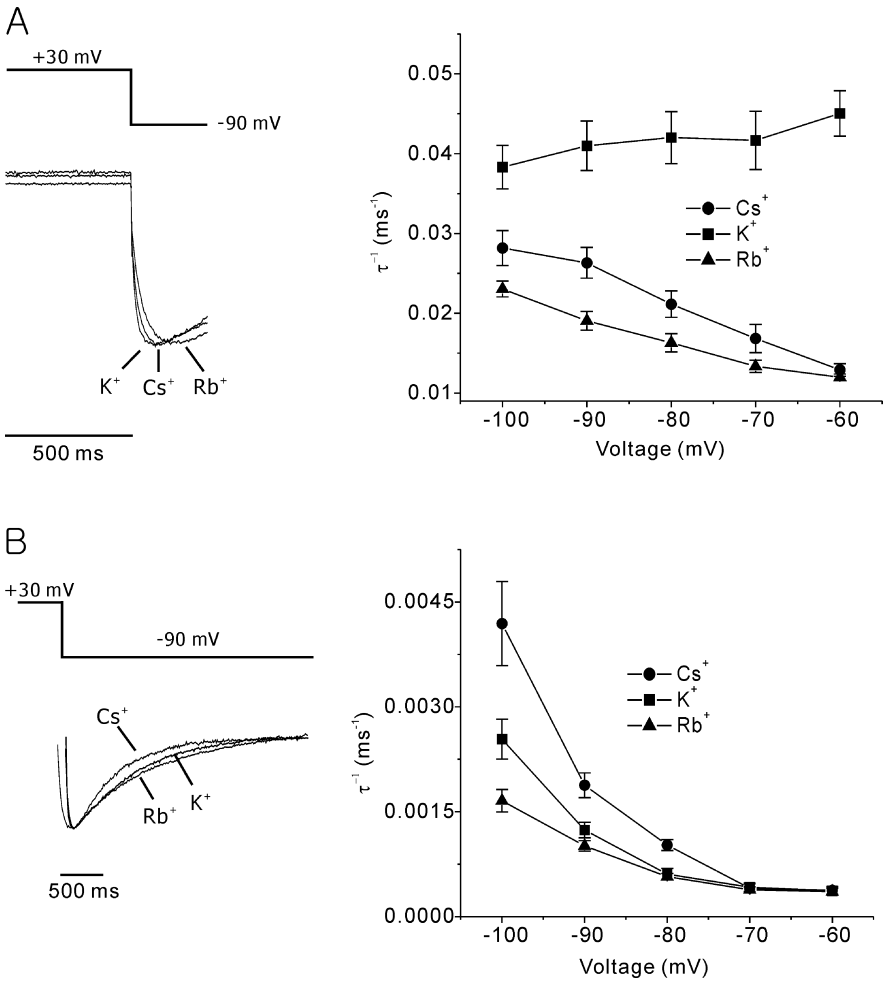

Fig. 5A, B Effects of external cations on the kinetics of deactivation and recovery from inactivation. Time constants of deactivation and recovery from inactivation were obtained by the step hyperpolarizing pulse protocol described in Fig. 1A. The rapid rising component of inward currents represents recovery from inactivation, while the slow relaxing component represents deactivation. Current traces in Cs_o^+, K_o^+, and Rb_o^+ were normalized to the maximum value and superimposed to compare the rate of recovery from inactivation (**A**, *left panel*) and deactivation (**B**, *left panel*). In the case of deactivation, current traces were superimposed from the point of time to peak to compare the time courses of deactivation. Current traces were fitted to a multiplication of two monoexponential functions to give the time constants. The reciprocals of the time constants of recovery from inactivation (**A**, *right panel*) and deactivation (**B**, *right panel*) were then plotted against test potential ($n = 5$)

dence of activation was not altered significantly in both studies.

To demonstrate the effect of altered inactivation on membrane currents, a model simulating HERG current in 140 mM K_o^+ (Fig. 6A, upper panel) was reconstructed with the activation and inactivation parameters obtained from the above results. Model formulation and parameters to reconstruct the HERG current are described in Appendix 1. When the voltage dependence of steady-state inactivation was shifted to a more positive membrane potential by 39 mV and the inactivation was slowed by four times (Fig. 6A, middle panel), the amplitude of the outward currents was increased by 60–70%. Slowing the inactivation by 20 times (Fig. 6A, lower panel) revealed the time-dependent rise and decay of outward currents more clearly. Peak current–voltage relationships (Fig. 6B) were also changed. The current–voltage relationship obtained from the conditions of altered inactivation showed a lower degree of inward rectification compared with that from control condition. Currents were very similar to those recorded from CHO cells bathed in 140 mM $[Rb^+]_o$ (compare the middle panel of Fig. 1A with that of Fig. 6A) or $[Cs^+]_o$ (compare the lower panel of Fig. 1A with that of Fig. 6A) with respect to the time course and current–voltage relationship. The current–voltage relationship obtained from CHO cells bathed in 140 mM $[Rb^+]_o$ (Fig. 1B), however, showed a high degree of inward rectification when compared with the simulation result (Fig. 6B). It is thought that the difference comes from the insufficient consideration of changes derived from cationic replacement. The simulation considered only the modulation of the inactivation gate by cationic replacement, but not changes of permeability characteristics.

The other interesting finding of the present study is that the HERG channel is not highly selective for K^+ but has significant permeability for Rb^+ and Cs^+. Ratios for P_{Rb}/P_K and P_{Cs}/P_K were 1.25 and 0.56, respectively (Fig. 1C). Cs^+ permeability for HERG-related channels was previously observed in HERG channels expressed in *Xenopus* oocytes (Schönherr and Heinemann 1996), I_{Kr} in rat atrial myocytes (Youm et al. 2000), *Drosophila eag* channels ($P_{Cs}/P_K = 0.42$) (Brüggemann et al. 1993), and, recently, in HERG channels expressed in a human embryonic kidney cell line, HEK 293 ($P_{Cs}/P_K = 0.36$) (Zhang et al. 2003). The mechanism underlying the poor selectivity for monovalent cations is not yet clear, but may be possibly explained by an analysis of the molecular structure of HERG channels. According to the crystal structure of KcsA, a model K^+ channel, hydro-

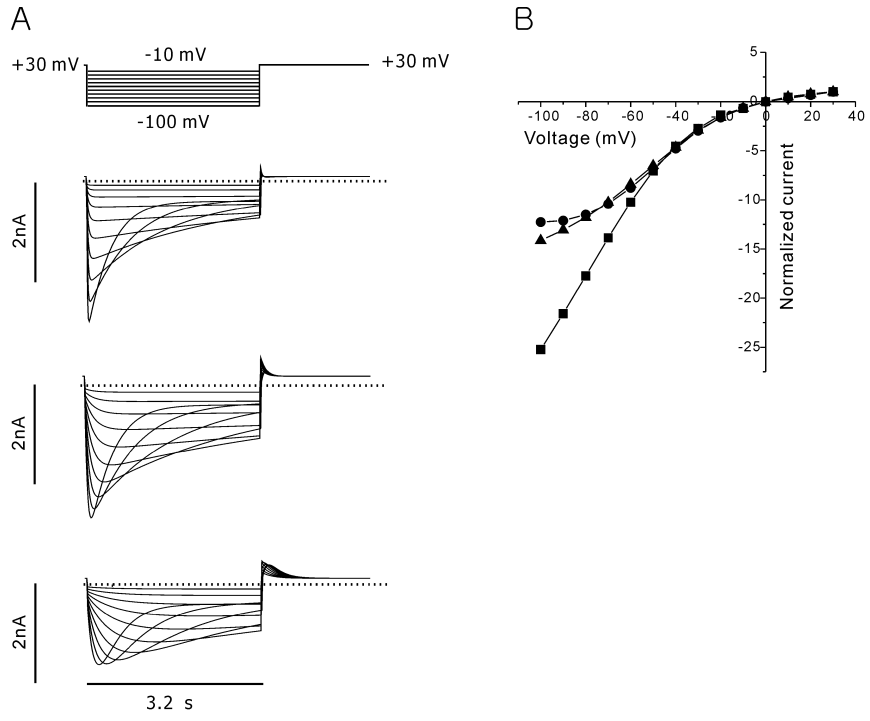

Fig. 6A, B Tracings of the computer simulation showing the result of altered inactivation. **A** Membrane currents were evoked by the same voltage clamp protocol described in Fig. 1A. The *upper panel* shows control simulated currents in 140 mM K_o^+; $[K^+]_i$ is 140 mM. Parameters and model formulations are demonstrated in the Appendix. *Middle and lower panels* show simulated currents by altered inactivation. To give the current tracings by altered inactivation, the voltage dependence of steady-state inactivation was shifted to positive membrane potential by 39 mV and inactivation time constants were slowed by 4 (*middle panel*) and 20 (*lower panel*) times, respectively. With these alterations of inactivation kinetics, outward tail currents appeared on return to the holding potential. Compare the tracings of membrane currents with those in Fig. 1A. For the middle and lower panels, following opening and closing rate constants of inactivation were used. *Middle panel*: $\alpha_h = 0.026 \exp\{(V+102.3)/(-24.7)\} + 0.0012 \exp\{(V+102.3)/(-4114.3)\}$, $\beta_h = 0.0006 \exp\{(V+88.3)/40.6\}$; *lower panel*: $\alpha_h = 0.0053 \exp\{(V+102.3)/(-24.7)\} + 0.00025 \exp\{(V+102.3)/(-4127.9)\}$, $\beta_h = 0.000197 \exp(V/38.1)$. **B** Current–voltage (*I–V*) relationships for the normalized amplitude of peak current at step hyperpolarization. Peak current amplitude was normalized to the value at +30 mV. *Filled squares*, *triangles*, and *circles* represent the normalized amplitude of peak current in the upper, middle, and lower panel of **A**, respectively. Actual current amplitude at +30 mV was 110 pA for filled squares, 188 pA for filled triangles, and 130 pA for filled circles

gen bonds can be formed around the outer mouth between the nitrogen atoms of "WW" and the hydroxyl groups of "Y" of the four subunits (Yellen 1998). In the HERG channel, the "WW" is replaced by "YF" (lacking nitrogen) and the "Y" is replaced by "F" (lacking hydroxyl groups). Therefore, hydrogen bonds are absent in the HERG channel, which will weaken molecular stability when the outer mouth is open (Tseng 2001). This will result in the outer mouth of the HERG channel being relatively narrower but more flexible, allowing entry of monovalent cations such as Cs^+, Rb^+, and Na^+. Entire replacement of K_o^+ with Na_o^+, however, failed to show inward Na^+ currents (data not shown). Furthermore, outward K^+ currents were not recorded on repolarization. One possible explanation is that, although Na_o^+ is able to enter the pore in the absence of K_o^+, it cannot exit and therefore occupies the channel, preventing outward flux of K_i^+. Further studies on ion selectivity and the molecular structure of the HERG channel should be performed to investigate the different behaviour of monovalent cations.

In the present study, we employed complete replacement of monovalent cations to show that inactivation gating is affected by ion species in extracellular solution. We only tested permeating ions with isotonic concentrations. The native channel, however, would be in a mixed ion environment, and the functional interaction between cations should be considered (Hagiwara and Takahashi 1974). In physiological conditions the major extracellular cation is Na^+, which is impermeable to HERG channels. Numaguchi et al. (2000) investigated the interaction of Na^+ and K^+ towards HERG channel by using the mole-fraction analysis, showing that extracellular Na^+ ions potently blocked the HERG current in K_o^+-free conditions, and K_o^+ in the physiological concentration range opposed the block by Na_o^+. They, however, mainly analyzed the effect of extracellular cations on current amplitude rather than activation or inactivation. It needs to be investigated in future studies whether extracellular cations in a physiological ion environment affect inactivation gating.

In conclusion, the results of the present study show that the HERG channel has poor selectivity for monovalent cations, with P_{Rb}/P_K of 1.25 and P_{Cs}/P_K of

0.56; the gating kinetics and voltage dependence of inactivation were affected most strongly by Cs^+ and to a lesser extent by Rb^+. These data support the concept that inactivation of the HERG channel shares the same "foot-in-the-door" model of gating as found in the *Shaker* K^+ channel. The dissociation between the order of permeability ratios ($Rb^+ > K^+ > Cs^+$) and the potency of affecting inactivation ($Cs^+ > Rb^+ > K^+$) among external cations requires further investigation of the physical interactions between cations and channel proteins in the permeation pathway.

Acknowledgements This work was supported by grants from the Korea Science and Engineering Foundation (971-0704-030-1) and from the Advanced Backbone IT Technology Development Project of the Ministry of Information and Communication (IMT-2000-C3-5).

Appendix

Appendix 1: model formulations for HERG channel

$$I_{HERG} = G_{HERG} mh(V - E_K)$$
$$G_{HERG} = 0.032$$
$$E_K = 0\ ([K^+]_i = 140\ mM,\ [K^+]_o = 140\ mM)$$
$$\alpha_m = 0.00425 \exp\{(V-23.3)/11.9\}$$
$$\beta_m = 0.00002 \exp\{(V+23.6)/(-15.4)\}$$
$$\alpha_h = 0.087 \exp\{(V-23.6)/(-100)\}$$
$$\beta_h = 0.033 \exp\{(V-32.7)/29.6\} + 0.015 \exp\{(V-32.7)/5064.6\}$$

Appendix 2: definition of symbols

I_{HERG}: HERG current (nA)

G_{HERG}: maximum conductance of HERG channels expressed in a CHO cell (μS)

m, h: activation and inactivation gates of HERG, respectively

α_m and β_m: opening and closing rate constants, respectively, of activation gate (ms^{-1})

α_h and β_h: opening and closing rate constants, respectively, of inactivation gate (ms^{-1})

V: membrane potential (mV)

E_K: reversal potential of K^+ (mV)

References

Baukrowitz T, Yellen G (1996) Use-dependent blockers and exit rate of the last ion from the multi-ion pore of a K^+ channel. Science 271:653–656

Brüggemann A, Pardo LA, Stühmer W, Pongs O (1993) *Ether-à-go-go* encodes a voltage-gated channel permeable to K^+ and Ca^{2+} and modulated by cAMP. Nature 365:445–448

Choi KL, Aldrich RW, Yellen G (1991) Tetraethylammonium blockade distinguishes two inactivation mechanisms in voltage-activated K^+ channels. Proc Natl Acad Sci USA 88:5092–5095

Curran ME, Splawski I, Timothy KW, Vincent GM, Green ED, Keating MT (1995) A molecular basis for cardiac arrhythmia: HERG mutations cause long QT syndrome. Cell 80:795–804

Escande D, Coulombe A, Faivre JF, Deroubaix E, Coraboeuf E (1987) Two types of transient outward current to repolarization in human atrium. Am J Physiol 252: H142–H148

Fan JS, Jiang M, Dun W, McDonald TV, Tseng GN (1999) Effects of outer mouth mutations on *hERG* channel function: a comparison with similar mutations in *Shaker*. Biophys J 76:3128–3140

Fedida D, Maruoka ND, Lin S (1999) Modulation of slow inactivation in human cardiac Kv1.5 channels by extra- and intracellular permeant cations. J Physiol (London) 515:315–329

Hagiwara S, Takahashi K (1974) The anomalous rectification and cation selectivity of the membrane of a starfish egg cell. J Membr Biol 18:61–80

Hamill OP, Marty A, Neher E, Sakmann B, Sigworth FJ (1981) Improved patch-clamp techniques for high-resolution current recording from cells and cell-free membrane patches. Pflügers Arch 391:85–100

Hille B (1992) Ionic channels of excitable membranes, 2nd edn. Sinauer, Sunderland, Mass., USA

Ho WK, Earm YE, Lee SH, Brown HF, Noble D (1996) Voltage- and time-dependent block of delayed rectifier K^+ current in rabbit sino-atrial node cells by external Ca^{2+} and Mg^{2+}. J Physiol (London) 494:727–742

Hoshi T, Zagotta WN, Aldrich RW (1990) Biophysical and molecular mechanisms of *Shaker* potassium channel inactivation. Science 250:533–538

Hoshi T, Zagotta WN, Aldrich RW (1991) Two types of inactivation in *Shaker* K^+ channels: effects of alterations in the carboxy terminal region. Neuron 7:547–556

Kiss L, Korn SJ (1999) Modulation of N-type Ca^{2+} channels by intracellular pH in chick sensory neurons. J Neurophysiol 81:1839–1847

Liu Y, Jurman ME, Yellen G (1996) Dynamic rearrangement of the outer mouth of a K^+ channel during gating. Neuron 16:859–867

Lopez-Barneo J, Hoshi T, Heinemann SH, Aldrich RW (1993) Effect of external cations and mutations in the pore region on C-type inactivation of *Shaker* potassium channels. Receptors Channels 1: 61–71

Marshall J, Molloy R, Moss GW, Howe JR, Hughes TE (1995) The jellyfish green fluorescent protein: a new tool for studying ion channel expression and function. Neuron 14:211–215

Numaguchi H, Johnson JP Jr, Petersen CI, Balser JR (2000) A sensitive mechanism for cation modulation of potassium current. Nat Neurosci 3:429–430

Ruben P, Thompson S (1984) Rapid recovery from K current inactivation on membrane hyperpolarization in molluscan neurons. J Gen Physiol 84:861–875

Sanchez-Chapula JA, Sanguinetti MC (2000) Altered gating of HERG potassium channels by cobalt and lanthanum. Pflügers Arch 440:264–274

Sanguinetti MC, Jurkiewicz NK (1990) Two components of cardiac delayed rectifier K current. J Gen Physiol 96:195–215

Sanguinetti MC, Jiang C, Curran ME, Keating MT (1995) A mechanistic link between an inherited and an acquired cardiac arrhythmia: HERG encodes the I_{Kr} potassium channel. Cell 81:299–307

Schönherr R, Heinemann SH (1996) Molecular determinants for activation and inactivation of HERG, a human inward rectifier potassium channel. J Physiol (London) 493:635–642

Shibasaki T (1987) Conductance and kinetics of delayed rectifier potassium channels in nodal cells of the rabbit heart. J Physiol (London) 387:227–250

Smith PL, Baukrowitz T, Yellen G (1996). The inward rectification mechanism of the HERG cardiac potassium channel. Nature 379:833–836

Spector PS, Curran ME, Zou A, Keating MT, Sanguinetti MC (1996) Fast inactivation causes rectification of the I_{Kr} channel. J Gen Physiol 107:611–619

Swenson RP Jr, Armstrong CM (1981) K^+ channels close more slowly in the presence of external K^+ and Rb^+. Nature 291:427–429

Trudeau MC, Warmke JW, Ganetzky B, Robertson GA (1995) HERG, a human inward rectifier in the voltage-gated potassium channel family. Science 269:92–95

Tseng GN (2001) I_{Kr}: the hERG channel. J Mol Cell Cardiol 33:835–849

Wang S, Morales MJ, Liu S, Strauss HC, Rasmusson RL (1996) Time, voltage and ionic concentration dependence of rectification of h-erg expressed in Xenopus oocytes. FEBS Lett 389:167–173

Wang S, Liu S, Morales MJ, Strauss HC, Rasmusson RL (1997) A quantitative analysis of the activation and inactivation kinetics of HERG expressed in *Xenopus* oocytes. J Physiol (London) 502:45–60

Yellen G (1998) The moving parts of voltage-gated ion channels. Q Rev Biophys 31:239–295

Youm JB, Zhang YH, Ho WK, Earm YE (1999) Physiologist 42: A-10

Youm JB, Ho WK, Earm YE (2000) Permeability characteristics of monovalent cations in atrial myocytes of the rat heart. Exp Physiol 85:143–150

Zagotta WN, Hoshi T, Aldrich RW (1990) Restoration of inactivation in mutants of Shaker potassium channels by a peptide derived from ShB. Science 250:568–571

Zhang S, Kehl SJ, Fedida D (2003) Modulation of human *ether-à-go-go*-related K^+ (HERG) channel inactivation by Cs^+ and K^+. J Physiol (London) 548:691–702

Zou A, Xu QP, Sanguinetti M (1998) A mutation in the pore region of HERG K^+ channels expressed in *Xenopus* oocytes reduced rectification by shifting the voltage dependence of inactivation. J Physiol (London) 509:129–137